

We are IntechOpen, the world's leading publisher of Open Access books Built by scientists, for scientists

6,900

Open access books available

186,000

International authors and editors

200M

Downloads

Our authors are among the

154

Countries delivered to

TOP 1%

most cited scientists

12.2%

Contributors from top 500 universities



WEB OF SCIENCE™

Selection of our books indexed in the Book Citation Index
in Web of Science™ Core Collection (BKCI)

Interested in publishing with us?
Contact book.department@intechopen.com

Numbers displayed above are based on latest data collected.
For more information visit www.intechopen.com



The Challenge of Controlling a Small Mars Plane

Seiki Chiba and Mikio Waki

Abstract

Dielectric elastomers (DEs) are lightweight and high-power, making them ideal for power control in a planetary exploration spacecraft. In this chapter, we will discuss the control of an exploration airplane exploring the surface of Mars using DEs. This airplane requires lightweight and powerful actuators to fly in the rare Martian atmosphere. DEs are a possible candidate for use as actuator controlling the airplane since they have high power, and high efficiency. A structural model of a wing having a control surface, a DE, and a linkage was built and a wind tunnel test of a control surface actuation using a DE actuator was carried out.

Keywords: mars airplane, control surface, dielectric elastomer, artificial muscle, actuator, high efficiency, high power, power control of planetary spacecraft, SWCNT

1. Introduction

Dielectric elastomer actuators (DEAs) are currently used in a variety of applications such as robots and medical devices. Since a DEA is very light and capable of high output, it is expected to be able to control the output of the planetary exploration ship and the solar panels loaded on exploration ships.

We are developing a DEA related to the output and control of Mars probes that observe the surface of Mars. Mars Airplane is a new Mars observation platform that enables a wide range of observations from low altitudes. Since 2010, the Japanese Mars spacecraft working group has been working on the conceptual design of Mars airplanes and various basic researches [1–5]. Mars exploration is performed with a weight of 6 kg, a wing width of 2.4 m, and a maximum cruising speed of 70 m/s. We are developing such a machine, as shown in **Figure 1** [6].

We would like to take this airplane down from the Mars exploration spacecraft with a parachute, disconnect the parachute at a high altitude (30 km) on Mars, control its flight remotely, and then gradually lower the altitude to fly a distance of about 300 km. Therefore, it is necessary to avoid high mountains on flights after the middle stage.

This Martian plane can obtain more detailed data than satellites and can observe a wider range than rovers. Also, one of the unique features of the Mars plane is to observe the formations of the canyons. Satellites cannot see the formation from the sky, and rovers cannot approach them.

Flight exploration by Martian planes has some difficulties, as detailed below:

These planes are not mass-produced and are very expensive due to their special payload and avionics for academic research. In addition to this, Mars planes must be

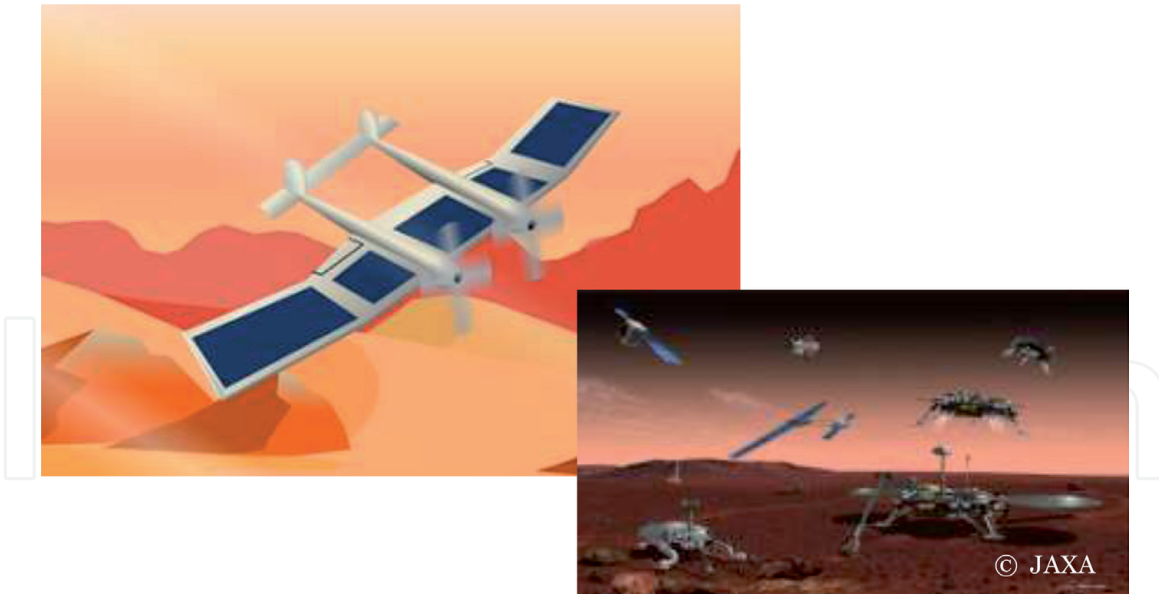


Figure 1.
Image of the Mars exploration airplane.

lightweight to fly in the thin atmosphere of Mars. It also has to be fairly lightweight to carry this spacecraft to Mars as well as to even be transported to Mars itself.

DEAs have the potential to be used as actuators for control surfaces (i.e. ailerons, rudder, and elevator) and as a propeller for the Mars airplane, since it is light and has high output and high efficiency. Another advantage of the DEA is that it is linearly driven, making it less susceptible to dust. This research investigated the feasibility of the DEA for the application of control surfaces (i.e., ailerons, rudder, and elevators) on the Mars airplane. A structural model of a wing having the control surface, the DEA, and a linkage was built, and a wind tunnel test of a control surface actuation using a DE actuator was carried out to investigate the feasibility of the DE actuators for the Mars airplane.

The results obtained in this study will be useful not only for the development of Mars exploration airplanes, but also for the structure and aerodynamic design of lightweight airplanes where large aerodynamic deformation is expected. The study also provides valuable examples of some of the expensive custom-made airplanes for academic research, airplanes that are not capable of many flight tests, and airplane development processes for which conducting flight tests are difficult.

2. Background of DE

To date, various types of soft actuators have been studied, and many functions desirable for different devices have been studied [7–31]. An especially attractive soft actuator is the dielectric elastomer (DE). DEs began to be studied in 1991 by R. Pelrine, S. Chiba et al. [16].

The basic element of a DE is a very simple structure comprised of a thin elastomer sandwiched by stretchable and flexible electrodes (see **Figure 2**) [24]. When a voltage difference is applied between the electrodes, they are attracted to each other by Coulomb forces leading to a thickness-wise contraction and plane-wise expansion of the elastomer. The typical thickness of the elastomers is about 500 microns to 1 mm. The electrode uses carbon black, CNT, or nano-sized metal. At the material level, the DE actuator has a fast speed of response (over 100,000 Hz), with a high strain rate (up to 680%), as shown in **Figure 3**, a high pressure, and a

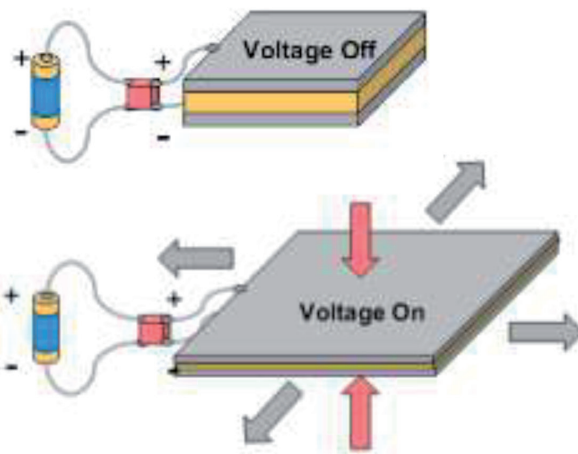


Figure 2.
Principle of operation of DEs.

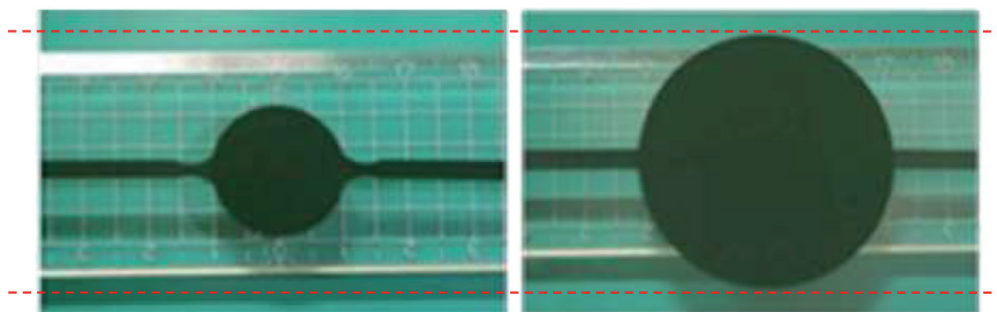


Figure 3.
Expanding Circular Actuator up to 680.

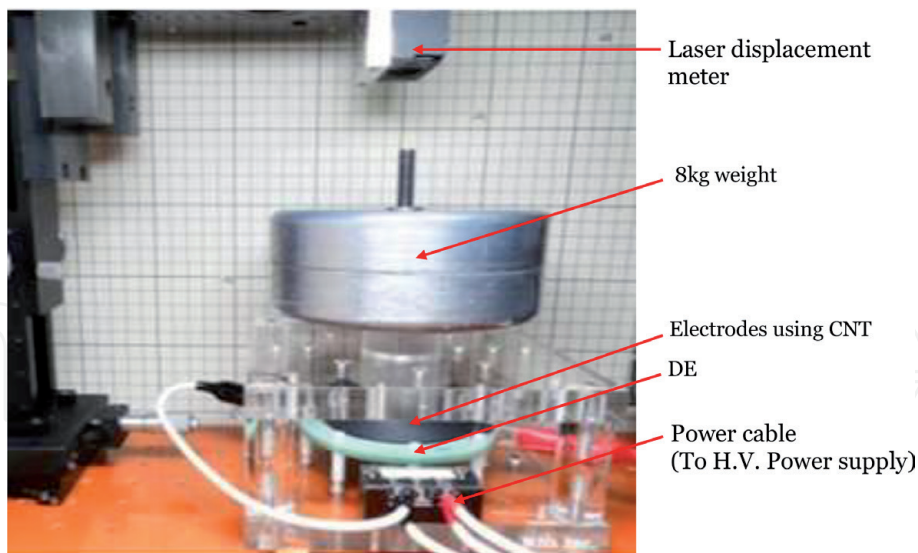


Figure 4.
A DE lifted a 8.0 kgf weight using SWCNTs (ZEONANO®-SG101) (ZEONANO®-SG101 is a single-wall carbon nanotube synthesized by the Super-Growth method. (Diaphragm type DE actuator having a diameter of 8 cm)).

power density of 1 W/g [32–34]. DEs can also be used for pressure-sensors and 3D position-sensors.

As shown in **Figure 4**, recently, DE actuators having only 0.15 g of DE material have been able to lift a weight of 8 kgf easily using the single wall carbon nano tube (SWCNT) electrodes (ZEONANO®-SG101) [33]. With 0.15 g of DEs, it is possible to lift an 8 kg weight by 1 mm or more. Its operating speed is 88 ms.

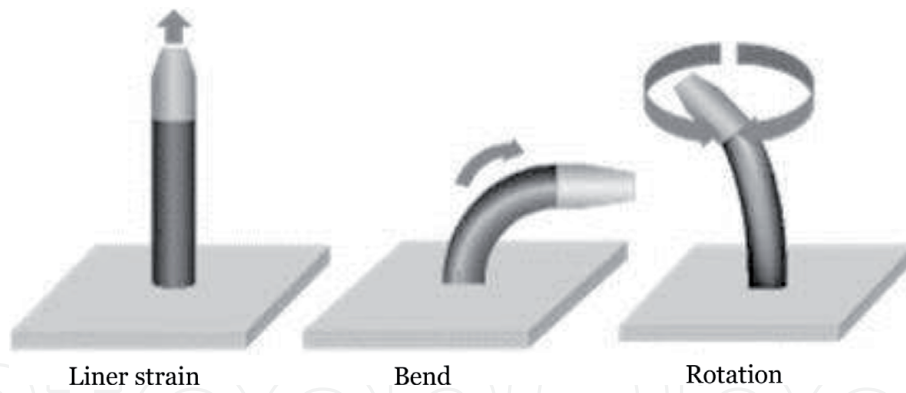
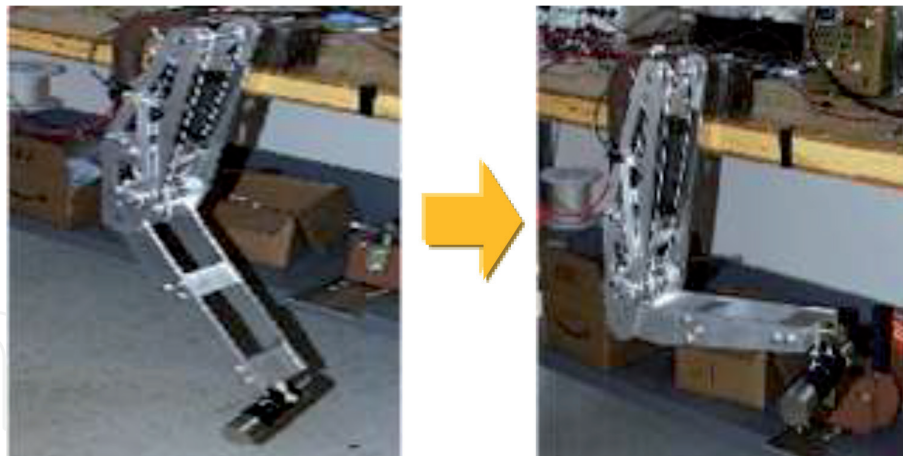


Figure 5.
Roll actuator having 3-DOF.



Leg robot



Robot arm

Figure 6.
Biologically inspired robots powered by DE rolls.

When the DE sheet is rolled, it becomes an actuator that looks like a human muscle. **Figure 5** shows the roll actuators with 3-DOF [34]. As shown in **Figure 6**, a DE can be the arm or leg of a robot. Using five of them, we created a robot that can move around the surface of Mars [34], so it enables sideways stepping like a crab without turning around, when it collides with wall.

These roll-type actuators seem to be ideal for moving the antenna or solar panel of a space craft to the correct position and as an actuator for a working robot arm on it. For example, a robot arm is attached to the Japanese experimental module



Figure 7.
International Space Station: Kibo (Japanese experiment module) has a robot arm.

Kibo of the International Space Station (see **Figure 7**). It is possible to use DEs as the drive source.

3. Experimental procedure

In order to verify the possibility of using a DEA as a surface control actuator for the Mars exploration airplane, a wind tunnel was used to operate with the DEA while receiving wind.

3.1 Experimental setup

Using a continuously circulating low-speed wind tunnel (see **Figure 8**) owned by JAXA (Japan Aerospace Exploration Agency), we conducted a verification

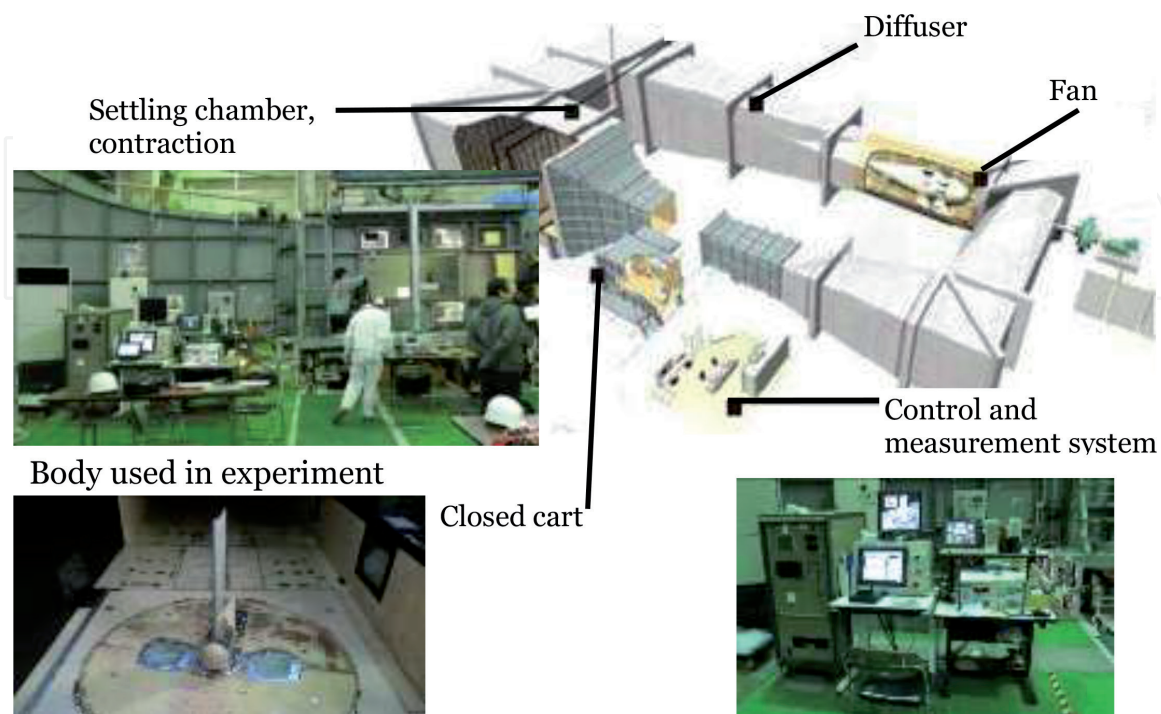


Figure 8.
2 m x 2 m Low-speed wind tunnel.

experiment to verify whether the DEA actuator could be used as a steering actuator under the wind received during flight. The wind tunnel used in this experiment has a measurement section of 2 m x 2 m and a maximum wind speed of 67 m / s (up to 60 m/s during continuous operation using the model).

In the preliminary study, the wind speed was set from 0 m/s to 40 m/s in order to match the actual driving conditions as much as possible. In addition, it was decided to observe the aileron driving state by changing the angle of attack from 0° to ±10° at 5° intervals at each wind speed (**Figure 9**).

The structural model of the wing used in the experiment was shaped vertically so that the surface control actuator (in this case, an aileron-like structure) can be driven by the DEA in a limited space in the wind tunnel. The body is shown in **Figure 10** [6].

The dimensions of the wings used in this experiment were 168.5 mm wide, 633 mm high and 25 mm thick, and the dimensions of the ailerons were 78.5 mm wide and 633 mm high. The wings and ailerons were made using polycarbonate resin for the frame and ABS resin for the exterior. The bottom of the model was 125 mm in diameter and 757.5 mm in length. The tip and tail are made of ABS resin,

Input parameters

Wind speed: 0 to 40 m/s (5 deg. increment)
 Angle of attack: -10 to +10deg (5 deg. increment)

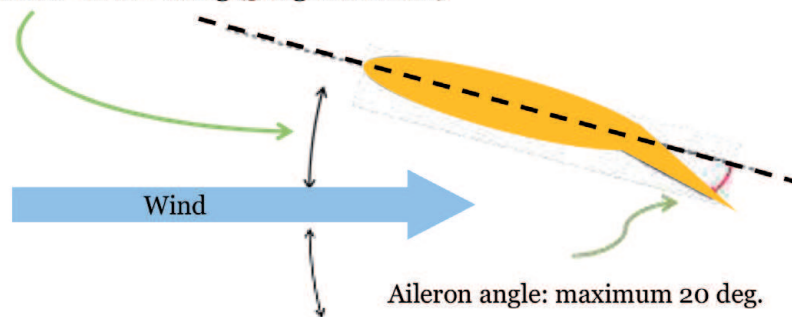


Figure 9.
 Input parameters.

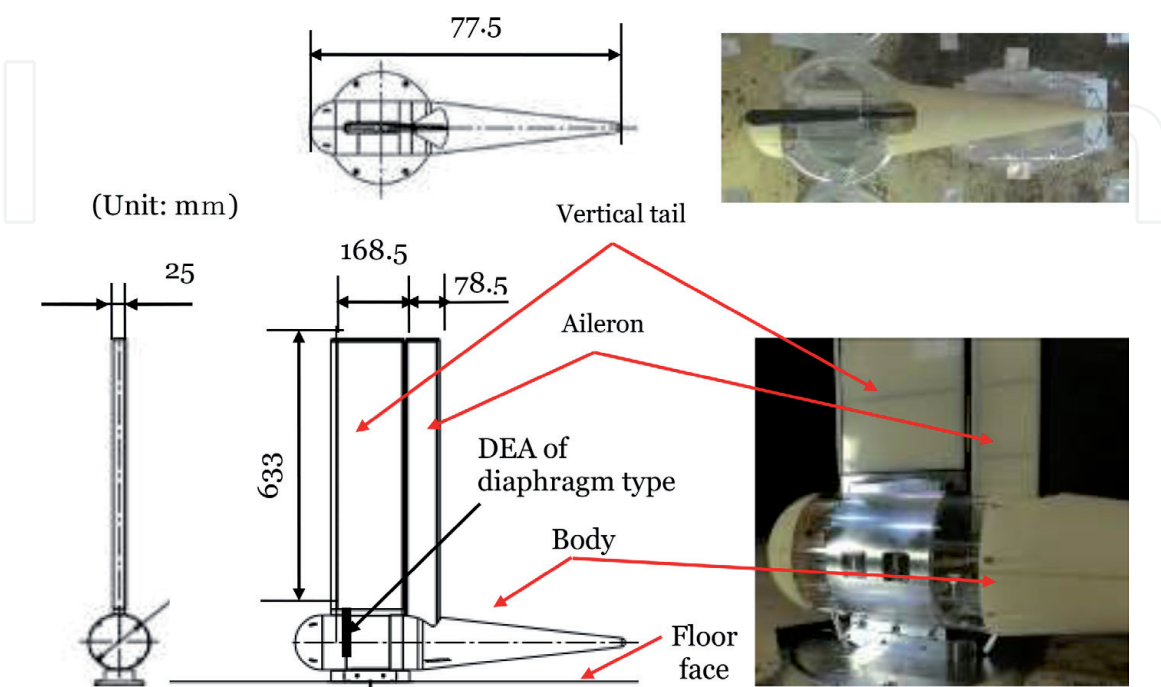


Figure 10.
 Body used in experiment.

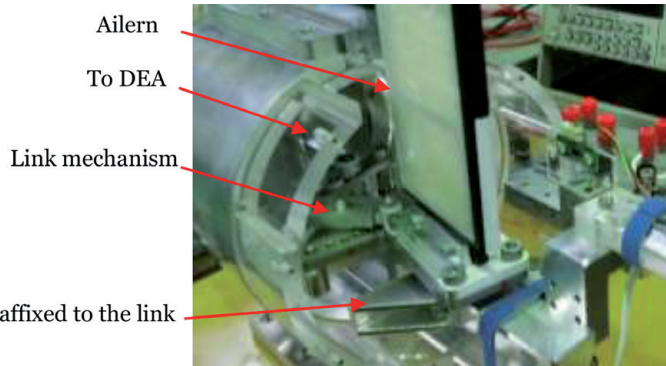


Figure 11.
 Link mechanism between the body and the measurement equipment.

and the center is made of acrylic resin. For strength, the parts are reinforced with aluminum. The aileron has a hollow structure, but the total weight was about 5 kg. A DEA to control ailerons was installed inside the body. The DEA and aileron are connected by a link mechanism built into the main body (see **Figure 11**) [6], and when the DEA is displaced by 2 mm, the aileron moves 20 degrees. The DEA unit for aileron drive has a structure that adopts a diaphragm type with an outer dimension of $\phi 100$ mm.

As shown in **Figure 12**, a load measuring device other than the main body, a high-voltage power supply, a high-voltage switch, etc. were installed outside the wind tunnel and connected to the main body with a cable so as not to obstruct the air flow in the wind tunnel [6]. A video camera was installed on the ceiling outside

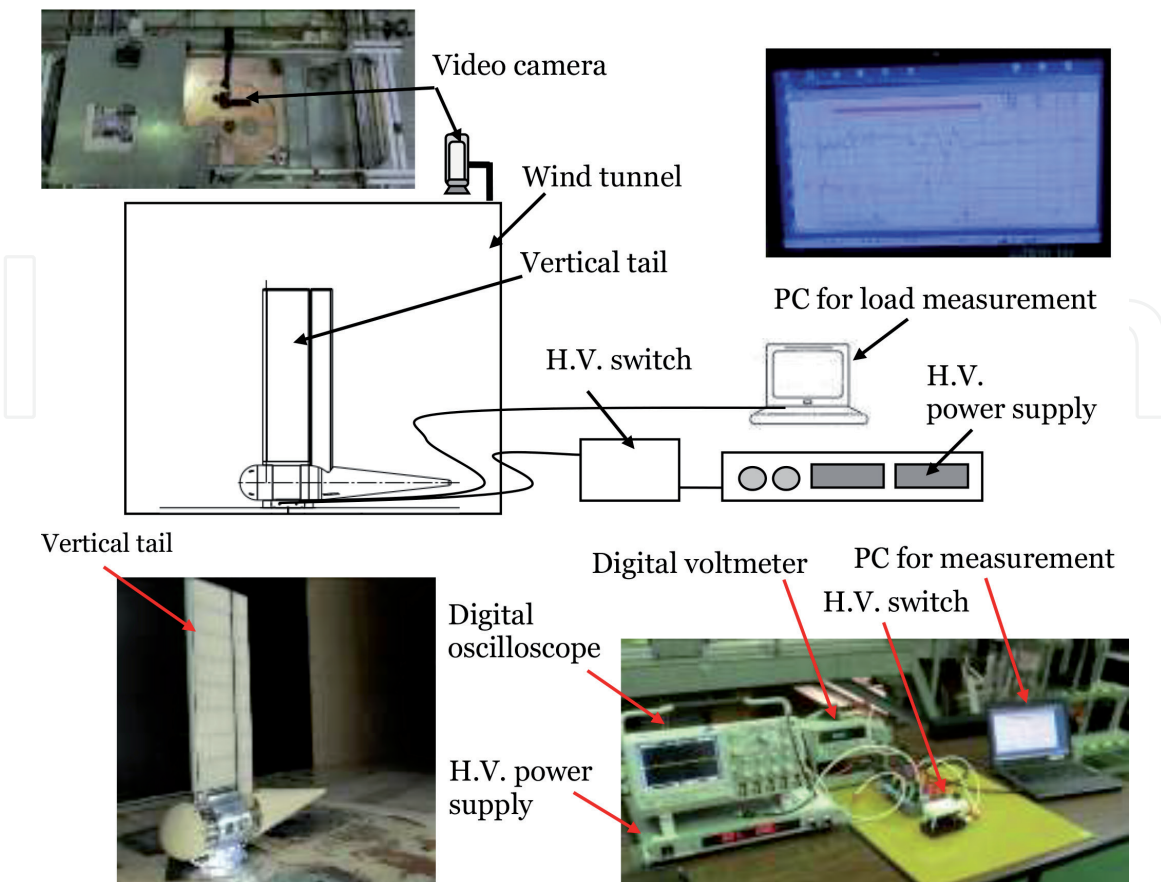


Figure 12.
 System diagram of the aileron drive experiment with a DEA.

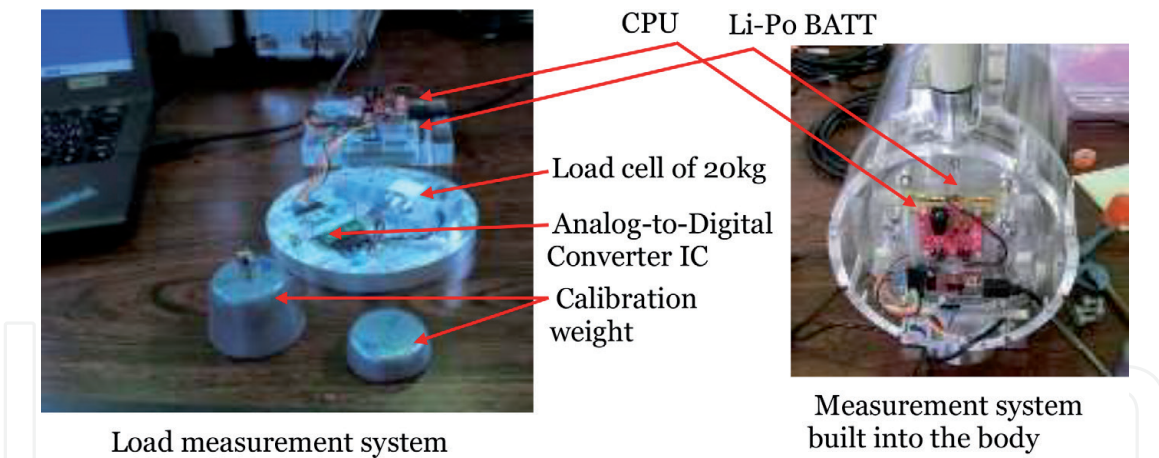


Figure 13.
Load measurement system using a load cell.

the wind tunnel to observe the state of the enclosure, and the images were taken from the observation window.

3.2 Preliminary experiment

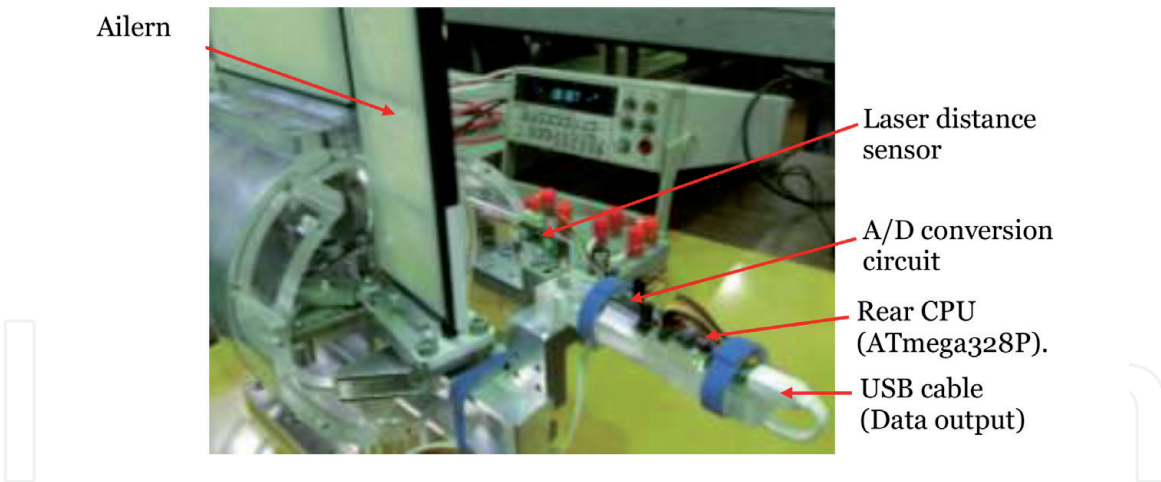
First, in order to examine the specifications required to control the actuator used to steer the aileron, a load cell was used to measure the load applied to the actuator part at each steering angle. **Figure 13** shows the measurement system used for load measurement [6].

The load cell used for load measurement was mounted at the DEA mounting position of the main body. The maximum load applied to the load cell is 20 kg, and the analog data output from the load cell is converted to digital data by the 24-bit A/D converter IC (HX-711), and the CPU (ATmega328P). A lithium polymer battery (Li-Po) was used as the power source to minimize the effect of noise on the weak signal output from the load cell. In order to shorten the connection distance, the circuit to the CPU was attached to the fuselage. A personal computer for operation and recording was installed outside the wind tunnel, and it was connected by serial communication.

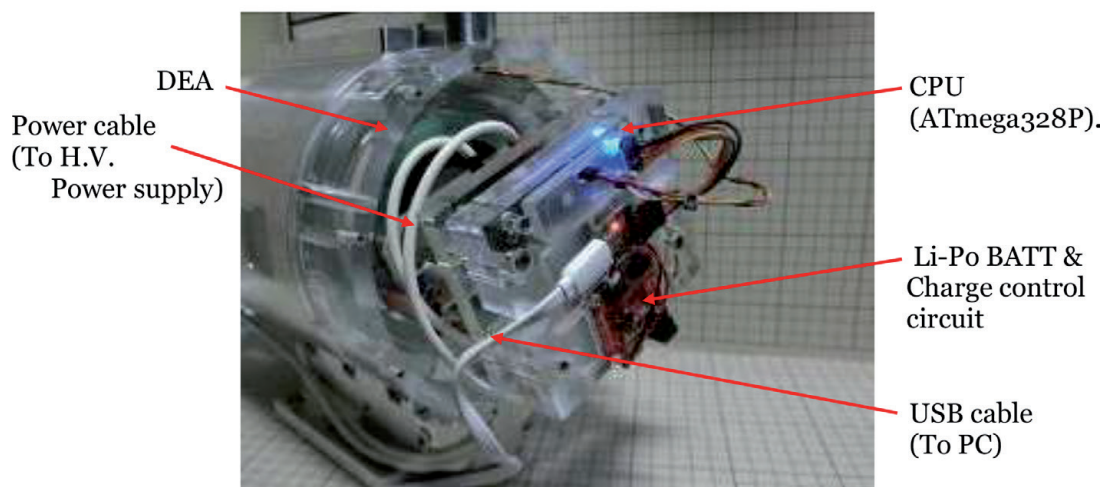
A laser distance sensor (VL50L0X) was also installed to measure the displacement velocity (**Figure 14**) [6]. Since this laser distance sensor uses I2C for the interface, it is not easily affected by noise and stable measurement is possible. The control was performed by the same CPU (ATmega328P) as the load measurement, and the measurement data was transmitted to the measurement PC by serial communication. Laser distance sensors were installed in the front and rear to observe the movement of ailerons and the DE.

The load was measured by continuously changing the wind speed from 0 m/s to 40 m/s in 5 m/s increments and setting the steering angles to 0, 5, 10, 15, and 20 degrees. When the set wind speed was reached, measurements were taken at each wind speed for about 30 seconds, and the load applied to the actuator section was measured (see **Figure 15**) [6].

In this experiment, it was found that the DEA was loaded with 11.54 kg/f in an environment with a steering angle of 20 degrees and a wind speed of 40 m/s (see **Table 1**). In order to move the aileron through the link mechanism, a force of about 2.6 kgf is required even in the absence of wind. It was found that a force of about 14.14 kg/f is required to steer 20 degrees in an environment with a wind speed of 40 m/s. It was also confirmed that the wings were deformed from the joint with the airframe at a wind speed of 30 m/s or more. Since the experiment was repeated in



a) Mounting location of the laser distance sensor



b) Laser distance sensor system

Figure 14.
 Laser distance sensor system installed inside the body. (a) Mounting location of the laser distance sensor;
 (b) Laser distance sensor system.

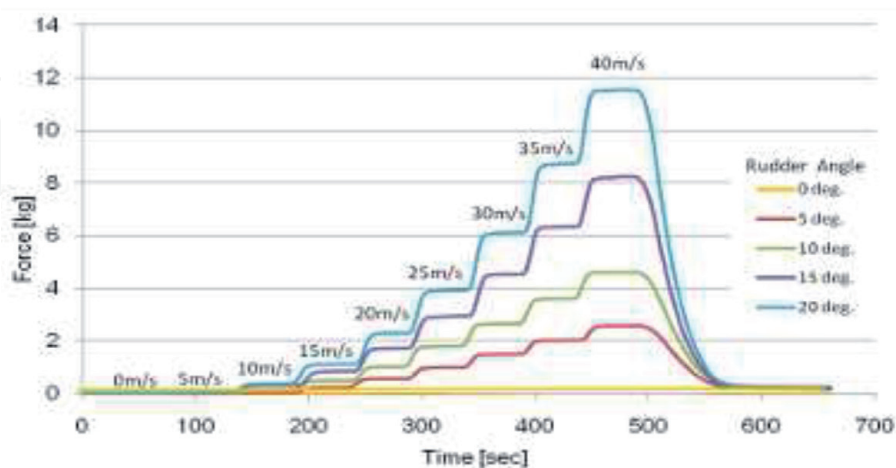


Figure 15.
 Load applied to the actuator section (by steering angle and wind speed).

such a state and there was a risk of damage to the blade due to fatigue, the aileron drive experiment with the DEA was carried out at a wind speed of 0 m/s to 30 m/s. In order to steer 20 degrees in this environment, a DEA that can obtain a force of about 8.7 kg/f is required.

	Wind speed (m/s)							
	5	10	15	20	25	30	35	40
Load applied to the actuator (kg / f)	0.12	0.37	1.12	2.30	3.90	6.10	8.72	11.54

Table 1.

Load applied to the actuator section at each wind speed when the rudder angle is 20 deg.

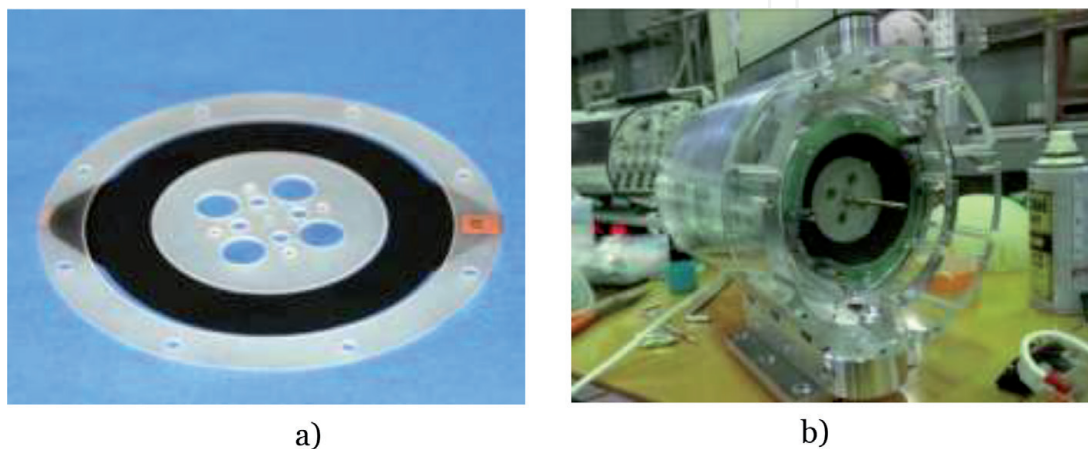
3.3 Aileron drive experiment with a DEA

The load cell mounted for load measurement was replaced with a diaphragm type DEA, and an aileron drive experiment was conducted. **Figure 16** shows the state of the DEA mounting.

The DEA unit used had a donut shape with an outer diameter of $\phi 100$ mm, a DEA part with an outer diameter of $\phi 80$ mm, and a central part of $\phi 50$ mm (see **Figure 15a**). The DEA used a 3 M acrylic sheet (VHB4910) as the main elastomer and SWCNT (SG101) manufactured by Zeon Corporation as the main electrode material. This DEA unit had a displacement performance of 2.0 mm with an applied voltage of DC 3.2 kV under a load of 4.0 kg, and the drive time at this time was about 100 ms. The DEA was driven by a high voltage power supply and a high voltage switch located outside the wind tunnel. The high-voltage power supply installed outside the wind tunnel and the DEA installed in the enclosure are connected by a high-voltage cable with a length of about 6 m. However, due to the low current consumption of the DEA, the maximum voltage drop during driving is 100 V, which is within the range where there is no problem in driving the DEA. The DEA unit consists of four cartridges, and if one of the DEA cartridges fails, the remaining DEA cartridges can drive it.

In this experiment, the wind speed was changed from 0 m/s to 20 m/s every 5 m/s, and the change in wind speed at each wind speed was recorded with a video camera installed on the ceiling of the wind tunnel. The rudder angle was measured by analyzing the recorded video.

In the initial experimental plan, the angle of attack was planned to be changed from -10° to $+10^\circ$ in 5° increments, but the stress applied to the wing was greater than expected, so there was a risk of damage to the skeleton. In order to avoid such an outcome, this time, the angle of attack was set to 0° only, and the wind speed was changed from 0 to 20 m/s at 5 m/s intervals.

**Figure 16.**

DEA mounted in the body. (a) Diaphragm type DEA. (b) DEA built into the body.

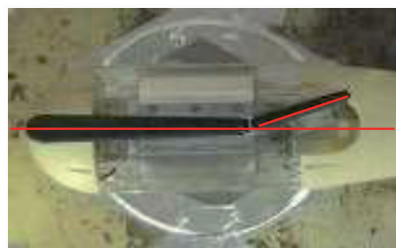
4. Results and discussion

Table 2 shows the aileron angle at each wind speed. **Figure 17** shows the aileron displacement at each wind speed [6]. Up to a wind speed of 5 m/s, the aileron angle could be obtained up to 20 deg. However, the aileron angle gradually decreased from a wind speed of 10 m/s and reached 4 deg. at a wind speed of 15 m/s.

Figure 18 shows the aileron drive speed when there is no wind, as measured in the lab. The rudder angle could be moved up to 20° at a speed of about 100 ms, and the same rudder angle and speed could be reproduced even if the drive control was repeated.

Aileron angle (deg.)	Wind speed (m/s)				
	0	5	10	15	20
	20	20	9	4	0

Table 2.
 Aileron angle at each wind speed.



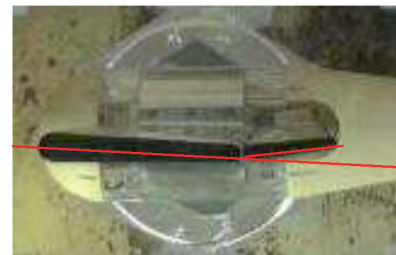
1) Wind speed: 0 m/s
 Aileron angle: 20 deg.



2) Wind speed: 5 m/s
 Aileron angle: 20 deg.



3) Wind speed: 10 m/s
 Aileron angle: 9 deg.



4) Wind speed: 15 m/s
 Aileron angle: 4 deg.

Figure 17.
 Aileron displacements at applied voltage DC_{3,200} V.

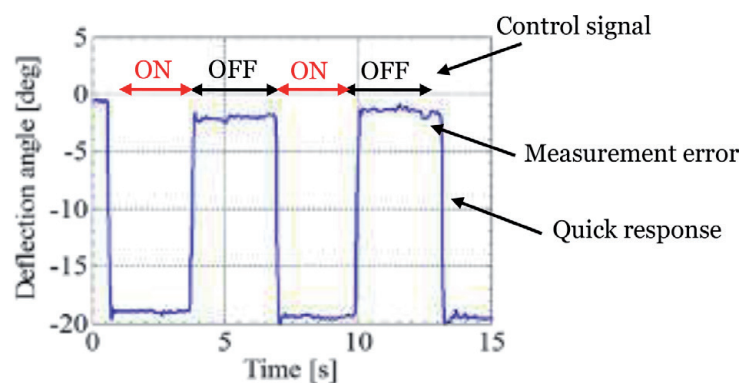


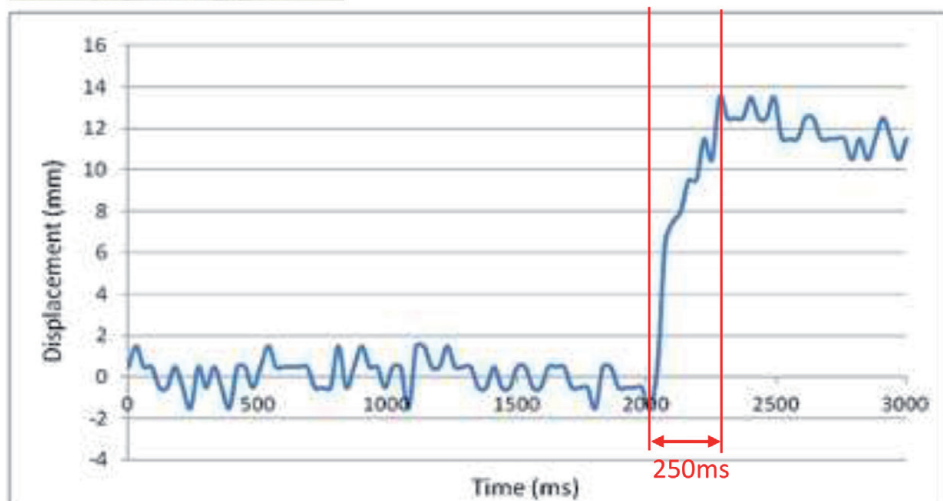
Figure 18.
 Aileron drive speed when there is no wind.

Figure 19 shows the operating speed of the aileron. The displacement speed was measured using a laser distance sensor mounted inside the body. At a wind speed of 5 m/s, it took 250 ms to reach the maximum displacement, but at a wind speed of 10 m/s, it took 300 ms. As described above, since the angle change of the aileron can be easily replaced with the voltage change, the feedback control can be easily performed by changing the voltage applied to the DEA using the voltage change.



Aileron angle at a “5 m/sec wind” condition

The aileron angle at a wind speed of 5 m / s was 20deg. The applied voltage at this time was 3.2kV. The operating speed was as fast as 250 ms.

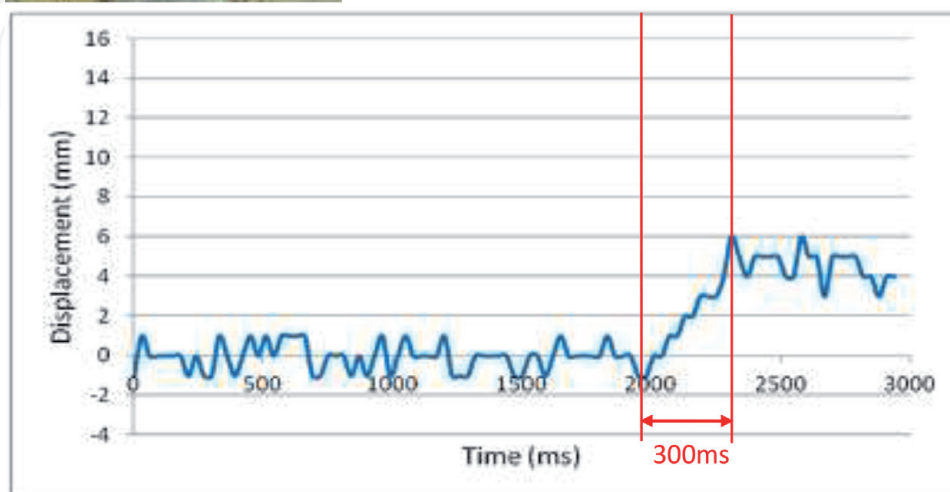


a)



Aileron angle at a “10 m/sec wind” condition

The aileron angle at a wind speed of 10 m / s was 9 deg. The applied voltage at this time was 3.2kV. The operating speed was as fast as 300 ms.



b)

Figure 19. Aileron's operating speed measured by the laser distance sensor. (a) Wind speed of 5 m/s; (b) Wind speed of 10 m/s.

The structural model used this time required a force of 2.6 kg for steering even at a wind speed of 0 m/s. This was a huge loss. It is probable that the maximum aileron angle could not be obtained due to insufficient driving force at a wind speed of 10 m/s. Most of this loss was due to the link mechanism. By increasing the efficiency of the link mechanism, we were able to obtain a maximum displacement of up to 15 m/s even with the same DEA. In the next experiment, we will investigate how much the mechanism can reduce the power consumed by developing a new drive that drives ailerons directly, enabling a simple and practical steering system.

To send a Martian plane to Mars, we need to dramatically reduce the weight of our compact and powerful motors. In addition, a powerful, efficient and responsive motor is essential for long-term flight of the spacecraft on the surface of Mars. Also, the surface temperature of Mars is very low and dust is present. Therefore, the required level of efficiency and responsiveness is very high. In this paper, based on the data obtained in this experiment, we attempted to compare the current level of a DEA with existing motors for these requirements.

First, we will explain the performance of the DE developed for this experiment:

The total weight of the DEA used is 52.8 g, of which 51.8 g is the weight of structures, etc., and the weight of the DEA itself is as small as 0.98 g. This DEA can lift a 4 kgf weight by 2 mm with an applied voltage of 3.3 kV. In order to increase this operating speed, the DE has been strengthened, and the total weight is 0.98 g, which is 98 ms.

Next is a comparison between the DE and existing motors:

From the above data, the power of the DE linear actuator is 0.0074 W per gram. As shown above, the weight including the DE actuator and its associated structure was approximately 53 g. If a similar linear actuator is configured using an existing DC motor of similar weight, the output of the linear actuator is 0.0015 (W). The weight including the DC motor and linear gear is about 95 g. Therefore, the DEA has a working speed per gram that is 4.9 times faster than a linear actuator that uses an existing DC motor. However, in the case of a linear actuator that uses a DC motor, a displacement of 1 mm takes about 200 milliseconds, so the difference in drive time is 9.9 times. In this experiment, we created a DE actuator that can lift a weight of 4 kgf using SWCNT (ZEONANO®-SG101) from Zeon Corporation. However, using high-crystal SWCNTs (extracted in the laboratory of Zeon Corporation under the guidance of Chiba et al.) gives about 1.32 times better results [35]. An SEM photograph of high-crystal CNTs is shown in **Figure 20**. It is estimated that DE motors using this CNT are about 13.1 times better than existing

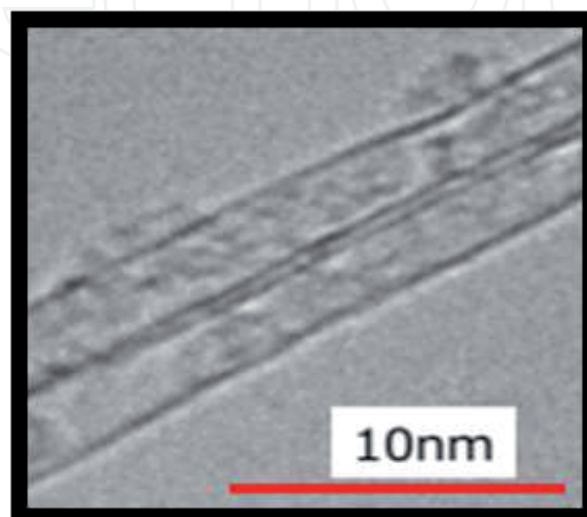


Figure 20.
SEM photograph of high-crystal CNT.

motors. When using metal CNTs, it is estimated to be twice as high as SWCNTs with high crystallinity. It is expected to be about 27.5 times that of existing motors.

In order to explain in more detail the good response of the DE obtained in this research, we compared it with the existing servo motor (which shows better performance than the model airplane used for radio control). The reason we chose the servo motor is that it can be controlled more accurately. The specifications of the servo motor that can obtain the same level of output as the DEA unit used this time are “servo motor (GWS): weight 41 g, torque 4.1 kg/cm, running speed: 270 ms/60 degrees”. In contrast, the DEA used this time weighs 36 g (when four cartridges are built in), is about 13% lighter than the servo motor, and has a drive speed of 98 ms/2 mm, so it can be driven at higher speeds.

Based on the data obtained, the power consumption of the DE will be explained as follows. The power consumption during driving was measured with a voltage/current monitor of a high-voltage power supply installed outdoors. The wind speed was 5 m/s, the applied voltage was 3.2 kV, and the power consumption was 0.29 W. The current at this time was as small as 0.09 mA, and there was almost no voltage drop or heat generation due to the wiring cable. As mentioned above, one of the features of the DEA is that it consumes less current and can contribute to the weight reduction of the wiring cable, that is, the weight reduction of the main body. The power consumption during driving was measured with a voltage/current monitor of a high-voltage power supply installed outdoors. The wind speed was 10 m/s, the applied voltage was 3.2 kV, and the power consumption was 0.29 W. The current at this time was as small as 0.09 mA, and there was almost no voltage drop or heat generation due to the wiring cable. One of the features of the DEA is that it consumes less current. It can also contribute to the reduction of wiring cables and reduce the weight of the aircraft.

Considering the manufacturing cost of a DE, the weight of the DE including reinforcement is 0.96 g, which is cheaper and lighter than the price of a general existing motor with the same output. The SWCNT used as the electrode material for the DE in this experiment has started being mass produced at ZEON, so it costs about 1,000 yen (\$9.6) per gram. Also, since the amount used is about 0.1 g, it is 100 yen (9 cents). The 3 M acrylic used for the elastomer is 20 yen per gram, so even if 1 g is used, it costs 120 yen (\$1.15), which is cheap enough. Also, as mentioned above, the DEA itself is sufficiently lightweight and compact, which is a great advantage when mounted on a rocket.

When the DE is actually transported to Mars, it passes through outer space, so the effects of cosmic rays cannot be ignored. Next year, we plan to conduct a DE exposure test at the International Space Station (ISS: see **Figure 7**) and observe its effects.

Finally, we will explain the further improvement of the DE. As shown in **Figure 4**, we succeeded in launching a weight of 8 kg with a DE of 0.15 g. Using this, it will probably be able to move smoothly even in the wind with a higher speed. In this experiment, SWCNT (SG101) was also used, but it has been found also that the use of highly crystallized SWCNTs further improves drive speed and output. Even if the above link mechanism is not improved significantly, wind experiments of 25 m/s or more can be performed. In addition, new acrylics are currently being synthesized by Chiba et al. These acrylics can be used at -40°C to 150°C and may be able to handle even the harsh temperatures found on Mars. Also, due to the sufficient withstand voltage of the film, the control unit of the Mars probe will be developed mainly using this elastomer.

5. Results and discussion

From the above experimental results, it is suitable for controlling the Mars probe because it can output a large amount of DE even with a small number of DEs and

has a high operating speed. In addition, DEs are manufactured at low manufacturing cost and can withstand -40°C .

Thus, for the first time in the world, we aim to fly in the atmosphere of Mars. By doing so, we would like to obtain our own Mars observation data such as high-resolution residual magnetic field data and atmospheric data. By establishing this technology, it will lead to the flight of other celestial bodies (Titan, Venus, etc.) that have an atmosphere.

The function of detecting radiation on Mars (particle type, energy range, dose range, etc.) and the function of detecting underground features such as caves and water volume, which are important considerations for Martian colonies, have not been considered in the paper. At this moment, the payload of the airplane is small and we will not be able to consider them. As mentioned in the background of DEs, however, the output of the DE has come to lift 8 kg against the weight of the 0.15 g DE. In the near future, we would like to increase the output of the DE, so that a larger payload can be realized.

DEs are also suitable for controlling the solar panels, antenna control, and drive output control of planetary exploration spacecraft.

What we need to know in the future is how well DEs can withstand cosmic rays. As early as next year, we plan to experiment with how a DE behaves in space on the International Space Station.

Recently, more and more research has been aimed at exploring the possibility of applying DEs to frequently used items such as spacesuits, power suits, and robots, and we hope that the results of this research will be valuable.

Acknowledgements

We would like to thank to Mr. Hiroki Ura and Mr. Takashi Yajima of the Aerodynamics Research Unit, Japan Aerospace Exploration Agency (JAXA)'s Ministry of Education, Culture, Science and Technology's Advanced Research Platform Operation Promotion Project "Wind and fluid Engineering Platform" for their enthusiastic support in getting this important data using their wind tunnel.

We also thank Aisin AW Co., LTD. for its financial support and manpower support during measurement in the wind tunnel.

Author details

Seiki Chiba^{1*} and Mikio Waki²

¹ Chiba Science Institute, Yagumo, Meguro Ward, Tokyo, Japan

² Wits Inc., Oshiage, Sakura, Tochigi, Japan

*Address all correspondence to: epam@hyperdrive-web.com

IntechOpen

© 2020 The Author(s). Licensee IntechOpen. This chapter is distributed under the terms of the Creative Commons Attribution License (<http://creativecommons.org/licenses/by/3.0>), which permits unrestricted use, distribution, and reproduction in any medium, provided the original work is properly cited. 

References

- [1] Nagai H, Oyama A: Mars Airplane, W.G. (2013) Mission Scenario of Mars Exploration by Airplane. Proceedings of the 2013 Asia-Pacific International Symposium on Aerospace Technology. 2013; 8:1-3.
- [2] Fujita K, Luong R, Nagai H, Asai K: Conceptual Design of Mars Airplane, Trans. JSASS Aerospace Tech. Japan. 2012; 10: 28p.
- [3] Fujita K, Nagai H, Robustness Analysis on Aerial Deployment Motion of a Mars Airplane using Multibody Dynamics Simulation: Effects of Wing-Unfolding Torque and Timing, The Aeronautical Journal. 2017; 121,1238: 449-468, DOI: 10.1017/aer.2016.123.
- [4] Fujita K, Chiba S et al, Feasibility of artificial muscle for mars airplane. Aeron Aero Open Access J: 2018; 111: p213, DOI:10.15406/aaaj.2018.02.00052.
- [5] Fujita K, Oyama O, Kubo D, Kanazaki M, Nagai H, Wind Tunnel Test for Videogrammetric Deformation Measurement of UAV for Mars Airplane Balloon Experiment-1 (MABE-1), Journal of Flow Control, Measurement & Visualization. 2019; 7:87-100, DOI: 10.4236/jfcmv.2019.72007
- [6] Chiba S et al, The challenge of controlling a small Mars exploration plane, In Proc. of SPIE, (Smart Structures and Materials Symposium and its 22nd Electroactive Polymer Actuators and Devices (EAPAD) Conference); 2020: 1137506. DOI: 10.1117/12.2551042.
- [7] Katchalsky K, Rapid swelling and deswelling of reversible gels of polymeric acid by ionization. Experimentia, 1945; 5: 319-320.
- [8] Steinberget IZ et al, Mechanochemical engines, Nature; 1966: 210: 568-571.
- [9] Hamilen F et. al, Electrolytically active contractile polymer: Nature, 1965; 206:1149-1150.
- [10] Agolin FI, Gay FP, Synthesis and properties of azoaromatic polymers. Macromolecules 3: 349-351, 1970.
- [11] Osada Y, Sato Y, Mechanochemical energy conversion in a polymer membrane by thermo-reversible polymer-polymer interactions. Makromolekulare Chem 1975; 176: 2761-2764.
- [12] Tanaka T, Collapse of gel and the critical endpoint. Phys Rev Lett 40; 1978: 820-823.
- [13] Pei Q et. al, Electrochemical application of the bending beam method. 1. Mass transport and volume changes in polypyrrole during redox. J Phys Chem 1992; 96:10507-10514.
- [14] Okuzak H, Kunugi T, Adsorption – induced bending of polypyrrole, films and its application to chemomechanical rotor. J. Polymer Sci. Polymer Phys. 1996; 43:1747-1749.
- [15] Hirai T, Actuator materials from polymer gels. Polymer gels responding to electric and magnetic field. J. Matter Sci. Soc. Japan. 1995; 32:59-63.
- [16] Pelrine R and Chiba S, Review of Artificial Muscle Approaches, (Invited) Proc. Third International Symposium on Micromachine and Human Science, Nagoya, Japan. 1992 October: 1-9.
- [17] Yu Y et. al, Directed bending of a polymer film by light. Nature. 2003; 425:145.
- [18] Oguro K, Fujiwara N, Asaka K, Onishi K, Sewa S, Polymer electrolyte actuator with gold electrodes, Proceedings of the SPIE's 6th Annual International Symposium on Smart

Structures and Materials, SPIE. 1999; 3669: 64-71.

[19] Otero FT, J. M. Sansiñena, Soft and wet conducting polymers for artificial muscles, *Advanced Materials*. 1998;10,6: 491-494.

[20] Osada Y, Okuzaki H, Hori H, A polymer gel with electrically driven motility, *Nature*, 1992; 355: 242-244.

[21] Wani OM, Zeng Z, Wasylczyk P, A. Priimagi, Programming Photoresponse in Liquid Crystal Polymer Actuators with Laser Projector, *Journal Recommendation service*. 2017; DOI: [org/10.1002/adom.201700949](http://dx.doi.org/10.1002/adom.201700949)

[22] Lee J et al, Magnetic force enhancement in a linear actuator by air-gap magnetic field distribution optimization and design, *Finite Elements in Analysis and Design*. 2012; 58: 44-52.

[23] Chiba S, Dielectric Elastomers, In *Soft actuators*, Asaka K, Okuzaki H, editors, *Soft actuator*, Springer; 2014. p. 183-195: ISBN978-4-431-54766-2.

[24] Tomori H et al. Theoretical Comparison of McKibben-Type Artificial Muscle and novel Straight-Fiber-Type Artificial Muscle, *Int. J. Automation Technology* 2011: 5(4), 544

[25] Shintake J, Rosset S, Schubert B, Mintchev S, Floreano D, Shea H, DEA for soft robotics: 1-gram picks up a 60-gram egg, *Proc. SPIE 9430, Electroactive Polymer Actuators and Devices (EAPAD)*; 2015: 94301S, DOI: [10.1117/12.2084043](https://doi.org/10.1117/12.2084043)

[26] Anderson L, Gisby T, McKay T, O'Brien B, Calius E, Multi-functional Dielectric Elastomer Artificial Muscles for Soft and Smart Machines, *J. Appl. Phys*;2012: 112,4: 041101.

[27] Kovacs GM, Manufacturing polymer transducers: opportunities

and challenges, *Proc. of SPIE*; 2018:10594-10597.

[28] Pei Q, Dielectric Elastomers past, present and potential future, *Proc. of SPIE*; 2018:10594-10594.

[29] Pelrine R, Kornbluh R, Chiba S et al., High-field defomation of elasomeric dielectrics for actuators, *Proc. 6th SPIE Symposium on Smart Structure and Materials*; 1999: 3669, 149-161.

[30] Chiba S et al, Recent Progress on Soft Transducers for sensor Networks, In *Technologies and Eco-innovation towards Sustainability II*, Hu A, editor, Springer Nature; 2019: p285-298, DOI: [org/10.1007/978-981-13-1196-3_23](http://dx.doi.org/10.1007/978-981-13-1196-3_23).

[31] Chiba S et al, Elastomer Transducers, *Advances in Science and Technology*, Trans Tech Publication, Switzerland; 2016: 97, 61-74. ISSN: 1662-0356, Doi: [10.4028/www.scientific.net/AST.97.61](https://doi.org/10.4028/www.scientific.net/AST.97.61)

[32] Chiba S et al, Challenge of creating high performance dielectric elastomers, *Proc. of SPIE 2021 (Smart Structures and Materials Symposium and its 23rd Electroactive Polymer Actuators and Devices (EAPAD) Conference)*; 2021:1157-62

[33] Waki M, Chiba S, Elastomer Transducers, *Soft actuators*, Chapter 33, p 447-460, Springer, 2014, ISBN978-4-431-54766-2.

[34] Chiba S et al, Dielectric elastomer using CNT as an electrode, *Proc. of SPIE 2020 (Smart Structures and Materials Symposium and its 22nd Electroactive Polymer Actuators and Devices (EAPAD) Conference)*; 2020:113751C-2. DOI:[10.1117/12.2548512](https://doi.org/10.1117/12.2548512)